Inorg. Chem. **2004**, *43*, 6600–6608

Copper(III) and Vanadium(IV)–Oxo Corrolazines

Joseph P. Fox,[†] Bobby Ramdhanie,[†] Adelajda A. Zareba,[‡] Roman S. Czernuszewicz,[‡] and David P. Goldberg*,[†]

Departments of Chemistry, The Johns Hopkins University, Baltimore, Maryland 21218, and University of Houston, Houston, Texas 77204-5003

Received May 11, 2004

As part of our efforts to develop the transition metal chemistry of corrolazines, which are ring-contracted porphyrinoid species most closely related to corroles, the vanadium and copper complexes $(TBP)_8Cz(H)V^{IV}O$ (**1**) and $(TBP)_8CzCu^{III}$ (**2**) of the ligand octakis(*para-tert*-butylphenyl)corrolazine [$(TBP)_8Cz$] have been synthesized. The coordination behavior, preferred oxidation states, and general redox properties of metallocorrolazines are of particular interest. The corrolazine ligand in **1** was shown to contain a labile proton by acid/base titration and IR spectroscopy, serving as a –2 ligand rather than as the usual –3 donor. The oxidation state of the vanadium center in **1** was shown to be +4, in agreement with the overall neutral charge for this complex. The EPR spectrum of **1** reveals a rich signal consistent with a $V^{IV}(O)$ (d^1, $S = 1/2$) porphyrinoid species ($g_{xx} = 1.989$, $g_{yy} = 1.972$, $g_{zz} = 1.962$). The electrochemical analysis of **1** shows behavior closer to that of a porphyrazine than a corrolazine, with a positively shifted, irreversible reduction at –0.65 V (vs Ag/AgCl). Resonance Raman and IR data for **1** confirm the presence of a triply bonded terminal oxo ligand with $\nu(V^{16}O) = 975\ cm^{-1}$ and $\nu(V^{18}O) = 939\ cm^{-1}$. The copper complex **2** exhibits a diamagnetic ^1H NMR spectrum, indicative of a bona fide square planar copper(III) (d^8, low-spin) complex. Previously reported copper corroles have been characterized as copper(III) complexes which exhibit a paramagnetic NMR spectrum at higher temperatures, indicative of a thermally accessible triplet excited state ([(corrole$^{\bullet+}$)Cu^{II}]). The NMR spectrum for **2** shows no paramagnetic behavior in the range 300–400 K, indicating that compound **2** does not have a thermally accessible triplet excited state. These data show that the corrolazine system is better able to stabilize the high oxidation state copper center than the corresponding corroles. Electrochemical studies of **2** reveal two reversible processes at +0.93 and –0.05 V, and bulk reduction of **2** with $NaBH_4$ generates the copper(II) species $[(TBP)_8CzCu^{II}]^-$ **(2a)**, which exhibits an EPR signal typical of a copper(II) porphyrinoid species.

Introduction

Corrolazines are relatively new entries in the porphyrinoid family and are most closely related to the ring-contracted, fully aromatic corrole compounds. Both corrolazines[1−6] and corroles[6−11] impart enhanced stability to transition metals in high oxidation states, and this feature is one of their most interesting properties. For example, we have recently described the synthesis and isolation of a stable manganese(V)−oxo corrolazine complex at room temperature.[2] For comparison, the most stable porphyrin complex of the same type is only fleetingly observable by spectroscopy at room temperature.[12−14] Many metallocorroles have been reported

* Author to whom correspondence should be addressed. E-mail: dpg@jhu.edu.
[†] The Johns Hopkins University.
[‡] University of Houston.

(1) Ramdhanie, B.; Stern, C. L.; Goldberg, D. P. *J. Am. Chem. Soc.* **2001**, *123*, 9447−9448.
(2) Mandimutsira, B. S.; Ramdhanie, B.; Todd, R. C.; Wang, H. L.; Zareba, A. A.; Czernuszewicz, R. S.; Goldberg, D. P. *J. Am. Chem. Soc.* **2002**, *124*, 15170−15171.
(3) Ramdhanie, B.; Zakharov, L. N.; Rheingold, A. L.; Goldberg, D. P. *Inorg. Chem.* **2002**, *41*, 4105−4107.
(4) Wang, S. H. L.; Mandimutsira, B. S.; Todd, R.; Ramdhanie, B.; Fox, J. P.; Goldberg, D. P. *J. Am. Chem. Soc.* **2004**, *126*, 18−19.
(5) Ramdhanie, B.; Telser, J.; Caneschi, A.; Zakharov, L. N.; Rheingold, A. L.; Goldberg, D. P. *J. Am. Chem. Soc.* **2004**, *126*, 2515−2525.
(6) Gryko, D. T.; Fox, J. P.; Goldberg, D. P. *J. Porphyrins Phthalocyanines* **2004**, in press.
(7) Paolesse, R. In *The Porphyrin Handbook*; Kadish, K. M., Smith, K. M., Guilard, R., Eds.; Academic Press: New York, 2000; Vol. 2, pp 201−232.
(8) Sessler, J. L.; Weghorn, S. J. In *Expanded, Contracted, & Isomeric Porphyrins*; Baldwin, J. E., Magnus, P. D., Eds.; Elsevier Science Inc.: New York, 1997; Vol. 15, pp 11−125.
(9) Gross, Z. *J. Biol. Inorg. Chem.* **2001**, *6*, 733−738.
(10) Gryko, D. T. *Eur. J. Org. Chem.* **2002**, 1735−1743.
(11) Erben, C.; Will, S.; Kadish, K. M. In *The Porphyrin Handbook*; Kadish, K. M., Smith, K. M., Guilard, R., Eds.; Academic Press: New York, 2000; Vol. 2, pp 233−300.

10.1021/ic049384a CCC: $27.50
Published on Web 09/17/2004

to contain high-valent transition metal centers, including Fe(IV),[15−24] Co(IV),[5,25,26] and Mn(V).[2,4,27−30] The assignment of oxidation state in these compounds is complicated by the possibility of "noninnocent" participation of the corrole ligand, in which a π-cation-radical accompanied by a reduced state of the metal may be a significant contributing form to the electronic configuration.[17,24,31,32]

In addition to these intriguing redox properties, metallocorroles and metallocorrolazines have exhibited catalytic reactivity (e.g., epoxidation, sulfoxidation, cyclopropanation).[4,15,18,19,27,28,30,33−35] These initial studies suggest that these compounds are worthy of further development with regard to building more efficient and selective catalysts, as well as stabilizing high oxidation states and exhibiting novel physical properties. Corroles and corrolazines are also useful for studying the mechanism of porphyrinoid-catalyzed reactions in which high-valent intermediates are presumed to play important roles.[4,15]

In this report we describe the synthesis and detailed spectroscopic characterization of two new metallocorrolazines, $(TBP)_8Cz(H)V^{IV}O$ (**1**) and $(TBP)_8CzCu^{III}$ (**2**) [$(TBP)_8$-Cz = octakis(*para*-*tert*-butylphenyl)corrolazine]. These compounds are the first examples of copper and vanadium corrolazines. There have been, however, several copper corroles previously described in the literature. These molecules exhibit diamagnetic, singlet ground states at room temperature corresponding to (corrole)Cu^{III} complexes and paramagnetic, triplet excited states ([(corrole-π-cation-radical)Cu^{II}]) at higher temperatures.[36−39] Thus, the copper corroles seem delicately balanced between a "high oxidation state" versus "noninnocent ligand" description, and these findings motivated us to synthesize the copper corrolazine **2** and determine its electronic configuration. In contrast to the copper corroles, there has only been one vanadium−oxo corrole previously reported.[40] Given our particular interest in high-valent metal−oxo corrolazines[2,4] and the general lack of information regarding vanadium−oxo species in corrole chemistry, we were inspired to synthesize the vanadium−oxo corrolazine **1**. Complexes **1** and **2** have been characterized by a number of physical methods including UV−vis, NMR, FT-IR, resonance Raman (RR), and EPR spectroscopies and cyclic voltammetry. The oxidation states and spin states of **1** and **2** have been defined by a combination of these techniques, and these data allow for some interesting comparisons to be made with metallocorrole analogues as well as other metallocorrolazines. Furthermore, we have shown by UV−vis spectroscopy that **1** can undergo reversible deprotonation/reprotonation with the addition of a stoichiometric amount of base or acid, confirming the presence of a labile proton in neutral **1**. In addition, the copper(III) complex **2** was reduced with $NaBH_4$ to give the anionic, EPR-active corrolazine $[(TBP)_8CzCu^{II}]^-$ **(2a)**.

Experimental Section

Materials and Methods. The metal-free corrolazine $(TBP)_8CzH_3$ was prepared according to literature methods.[1] Reagents and solvents were purchased from commercial sources and used without further purification unless otherwise noted. Preparation and handling of air-sensitive materials was carried out either under an argon atmosphere using standard Schlenk techniques or in a Vacuum Atmospheres Co. VAC-AV-3 inert-atmosphere (<1 ppm O_2) glovebox under nitrogen atmosphere. Solvents and solutions were deoxygenated by either repeated freeze−pump−thaw cycles or by direct bubbling of argon through the solution for 20−30 min. Thin-layer chromatography (TLC) was performed using Aldrich silica gel 60 F254 precoated plates (0.25 mm thickness). Flash chromatography was performed using silica gel 60A (170−400 mesh) from Fisher Scientific.

Physical Measurements. NMR spectra were recorded on a Varian Unity FT-NMR instrument at 400 MHz (^{1}H). All spectra were recorded in 5-mm o.d. NMR tubes, and chemical shifts were reported relative to a 0.1% TMS internal standard. All NMR spectra were taken at 23 °C unless otherwise noted. UV−vis spectra were analyzed via a Hewlett-Packard 8453 diode array spectrometer.

(12) Groves, J. T.; Lee, J.; Marla, S. S. *J. Am. Chem. Soc.* **1997**, *119*, 6269−6273.
(13) Jin, N.; Groves, J. T. *J. Am. Chem. Soc.* **1999**, *121*, 2923−2924.
(14) Nam, W.; Kim, I.; Lim, M. H.; Choi, H. J.; Lee, J. S.; Jang, H. G. *Chem.−Eur. J.* **2002**, *8*, 2067−2071.
(15) Collman, J. P.; Zeng, L.; Decréau, R. A. *Chem. Commun.* **2003**, 2974−2975.
(16) Cai, S.; Walker, F. A.; Licoccia, S. *Inorg. Chem.* **2000**, *39*, 3466−3478.
(17) Simkhovich, L.; Goldberg, I.; Gross, Z. *Inorg. Chem.* **2002**, *41*, 5433−5439.
(18) Grodkowski, J.; Neta, P.; Fujita, E.; Mahammed, A.; Simkhovich, L.; Gross, Z. *J. Phys. Chem. A* **2002**, *106*, 4772−4778.
(19) Simkhovich, L.; Gross, Z. *Tetrahedron Lett.* **2001**, *42*, 8089−8092.
(20) Vogel, E.; Will, S.; Tilling, A. S.; Neumann, L.; Lex, J.; Bill, E.; Trautwein, A. X.; Wieghardt, K. *Angew. Chem., Int. Ed. Engl.* **1994**, *33*, 731−735.
(21) Steene, E.; Wondimagegn, T.; Ghosh, A. *J. Phys. Chem. B* **2001**, *105*, 11406−11413.
(22) Zakharieva, O.; Schünemann, V.; Gerdan, M.; Licoccia, S.; Cai, S.; Walker, F. A.; Trautwein, A. X. *J. Am. Chem. Soc.* **2002**, *124*, 6636−6648.
(23) Cai, S.; Licoccia, S.; Walker, F. A. *Inorg. Chem.* **2001**, *40*, 5795−5798.
(24) Walker, F. A. *Inorg. Chem.* **2003**, *42*, 4526−4544.
(25) Harmer, J.; Van Doorslaer, S.; Gromov, I.; Bröring, M.; Jeschke, G.; Schweiger, A. *J. Phys. Chem. B* **2002**, *106*, 2801−2811.
(26) Will, S.; Lex, J.; Vogel, E.; Adamian, V. A.; Van Caemelbecke, E.; Kadish, K. M. *Inorg. Chem.* **1996**, *35*, 5577−5583.
(27) Golubkov, G.; Bendix, J.; Gray, H. B.; Mahammed, A.; Goldberg, I.; DiBilio, A. J.; Gross, Z. *Angew. Chem., Int. Ed.* **2001**, *40*, 2132−2134.
(28) Liu, H. Y.; Lai, T. S.; Yeung, L. L.; Chang, C. K. *Org. Lett.* **2003**, *5*, 617−620.
(29) Eikey, R. A.; Khan, S. I.; Abu-Omar, M. M. *Angew. Chem., Int. Ed.* **2002**, *41*, 3592−3595.
(30) Gross, Z.; Golubkov, G.; Simkhovich, L. *Angew. Chem., Int. Ed.* **2000**, *39*, 4045−4047.
(31) Ghosh, A.; Steene, E. *J. Biol. Inorg. Chem.* **2001**, *6*, 739−752.
(32) Ghosh, A.; Steene, E. *J. Inorg. Biochem.* **2002**, *91*, 423−436.
(33) Gross, Z.; Simkhovich, L.; Galili, N. *Chem. Commun.* **1999**, 599−600.
(34) Mahammed, A.; Gray, H. B.; Meier-Callahan, A. E.; Gross, Z. *J. Am. Chem. Soc.* **2003**, *125*, 1162−1163.
(35) Simkhovich, L.; Mahammed, A.; Goldberg, I.; Gross, Z. *Chem.−Eur. J.* **2001**, *7*, 1041−1055.
(36) Ghosh, A.; Wondimagegn, T.; Parusel, A. B. J. *J. Am. Chem. Soc.* **2000**, *122*, 5100−5104.
(37) Wasbotten, I. H.; Wondimagegn, T.; Ghosh, A. *J. Am. Chem. Soc.* **2002**, *124*, 8104−8116.
(38) Kadish, K. M.; Adamian, V. A.; Van Caemelbecke, E.; Gueletii, E.; Will, S.; Erben, C.; Vogel, E. *J. Am. Chem. Soc.* **1998**, *120*, 11986−11993.
(39) Brückner, C.; Briñas, R. P.; Bauer, J. A. K. *Inorg. Chem.* **2003**, *42*, 4495−4497.
(40) Licoccia, S.; Paolesse, R.; Tassoni, E.; Polizio, F.; Boschi, T. *J. Chem. Soc., Dalton Trans.* **1995**, 3617−3621.

Mass spectra were collected at Johns Hopkins University with a VG analytical 70-S mass spectrometer in FAB ionization mode. Infrared spectra were measured either in KCl pellets at room temperature with a Nicolet Avator 360 FT-IR spectrometer or as a film on NaCl plates with a Perkin-Elmer RX I FT-IR. Electron paramagnetic resonance (EPR) spectra were obtained on a Bruker EMX EPR spectrometer controlled with a Bruker ER 041 X G microwave bridge. The low-temperature EPR measurements were carried out via either a continuous-flow liquid-helium cryostat and ITC503 temperature controller made by Oxford Intruments, Inc., or a liquid-nitrogen finger dewar. EPR simulations were performed with Win-SimFonia software made by Bruker BioSpin. Elemental analyses were performed by Atlantic Microlab, Inc., Atlanta, GA.

Vanadyl Octakis(*para-tert*-butylphenyl)corrolazine, $(TBP)_8Cz(H)V^{IV}O$ (1). To a stirring solution of $(TBP)_8CzH_3$ (280 mg, 0.21 mmol) in 30 mL of pyridine was added $VO(acac)_2$ (273 mg, 1.03 mmol). The solution was brought to reflux for 1 h and the solvent subsequently removed under vacuum. Purification by silica gel chromatography (CH_2Cl_2) afforded a brown solid (161 mg, 55%) with $R_f = 0.70$ (TLC, methylene chloride). ^{1}H NMR (400 MHz, CD_2Cl_2): 9.5−6.8 (broad resonance, 32H), 1.6−1.0 (m, 72H). UV−vis (CH_2Cl_2) [λ_{max}, nm ($10^{-4}\epsilon$)]: 435 (4.7), 465 (5.7), 543 (0.5), 655 (shoulder, 1.2) 710 (3.3). IR (thin film) (cm^{-1}; ν): 3354 (N−H), 2961, 2867, 1463, 1393, 1376, 1368, 1268, 1154, 1107, 1042, 1014, 994, 980 (V≡O), 875, 867, 827, 752, 606. FAB-MS [*m*/*z* (% intensity)]: 1424 (M + 1, 100). Anal. Calcd for $C_{96}H_{105}N_7VO\cdot CH_2Cl_2$: C, 77.22; H, 7.15; N, 6.49. Found: C, 77.43; H, 6.91; N, 6.44.

Copper(III) Octakis(*para-tert*-butylphenyl)corrolazine, $(TBP)_8CzCu$ (2). To a stirring solution of $(TBP)_8CzH_3$ (368 mg, 0.27 mmol) in 25 mL of pyridine was added cupric acetate (500 mg, 2.50 mmol). The solution was brought to reflux for 1 h and the solvent subsequently removed under reduced pressure. Purification by silica gel chromatography (CH_2Cl_2) afforded a blue-green solid (338 mg, 88%) with $R_f = 0.55$ (TLC, methylene chloride). ^{1}H NMR (400 MHz, CD_2Cl_2): 8.27 (app t, J = 7.6 Hz, 8H), 7.91 (d, J = 8.0 Hz, 4H), 7.61 (app d, J = 6.4 Hz, 8H), 7.44 (app d, J = 6.0 Hz, 8H), 7.15 (d, J = 7.2 Hz, 4H), 1.45 (s, 18H), 1.44 (s, 18H), 1.37 (s, 18H), 1.32 (s, 18H). UV−vis (CH_2Cl_2) [λ_{max}, nm ($10^{-4}\epsilon$)]: 440 (1.5), 645 (0.9). IR (thin film) (ν; cm^{-1}): 2954, 2924, 2855, 1463, 1363, 1267, 1200, 1165, 1106, 1015, 993, 868, 837, 761, 700, 620, 564. FAB [*m*/*z* (% intensity)]: 1420 (M + 1, 100). Anal. Calcd for $C_{96}H_{104}N_7Cu\cdot 3CH_2Cl_2$: C, 71.02; H, 6.62; N, 5.85. Found: C, 71.07; H, 6.57; N, 5.80.

Resonance Raman Spectroscopy of 1. Excitation radiation (457.9 and 488.0 nm) near the absorption maxima of the Soret band (435/465 nm) was provided by a Coherent 90-6 Ar^+ ion laser. The ^{18}O-substituted $(TBP)_8Cz(H)V^{IV}O$ (**1**) was prepared by equilibrating millimolar samples dissolved in CH_2Cl_2 (1 mL) with ∼20 μL of pure $H_2{}^{18}O$ (97 at. % ^{18}O, Isotec, Miamisburg, OH) for 12 h followed by complete evaporation to dryness of the solvent under vacuo. The scattered photons were collected via frontscattering (135° illumination angle) geometry from spinning samples in pressed KCl pellets[41] (solid samples) or NMR tubes[42] (CH_2Cl_2 solutions) at room temperature with 50 (solids) and 70 mW (solutions) laser powers and 4 cm^{-1} slit widths. All RR spectra were acquired under the control of a Spex DM3000 microcomputer system using a scanning Raman instrument equipped with a Spex 1403 double monochromator (with a pair of 1800 grooves/mm gratings) and a Hamamatsu 928 photomultiplier detector, as described in details elsewhere.[43] To improve the signal-to-noise ratio multiple scans (7−13 scans) were collected and then averaged. The slowly sloping baselines were subtracted from the digitally collected spectra by using GRAMS/32 software package (Thermo Galactic, Inc.). An IGOR Pro (version 4.0) software was used to prepare the spectral figures. The absorption spectra were obtained before and after the RR measurements on a Cary 50 spectrophotometer in 0.1 mm quartz cuvettes using CH_2Cl_2 as a solvent to ensure the integrity of the sample.

Scheme 1[a]

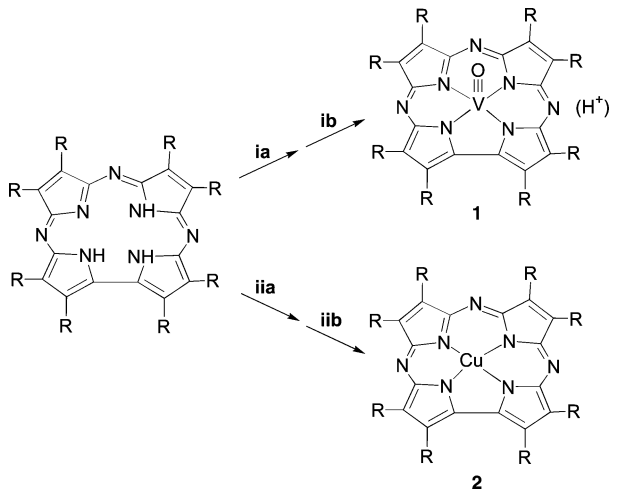

[a] Reagents and conditions: (ia) $VO(acac)_2$, pyridine, 118 °C, 1 h; (ib) silica gel column, CH_2Cl_2 (eluent) (62%); (iia) $Cu(OAc)_2$, pyridine, 118 °C, 1 h; (iib) silica gel column, CH_2Cl_2 (eluent) (88%).

Electrochemistry. Cyclic voltammograms were measured with an EG&G Princeton Applied Research potentiostat/galvanostat model 263A at scan rates of 0.5−0.025 V s^{-1}. A three-electrode configuration made up of a platinum working electrode, a Ag/AgCl reference electrode (3.5 M KCl), and a platinum wire auxiliary electrode was employed. Measurements were performed at ambient temperatures under nitrogen with 0.10 M TBAP (TBAP = tetra-*n*-butylammonium hexafluorophosphate, recrystallized 3 times from ethanol and stored in a vacuum oven at 50 °C for 5 days prior to analysis) as the supporting electrolyte in CH_2Cl_2. The ferrocenium/ferrocene couple ($FeCp_2{}^{+/0}$) at 0.45 V was used as the external reference.

Results and Discussion

Synthesis of $(TBP)_8Cz(H)V^{IV}O$ (1) and $(TBP)_8CzCu$ (2). Synthesis of the vanadium−oxo complex **1** was accomplished via treatment of metal-free $(TBP)_8CzH_3$ (0.21 mmol) with a 5-fold excess of vanadyl acetylacetonate in refluxing pyridine for 1 h (Scheme 1). The crude product was isolated as a brown residue after removal of the solvent by vacuum distillation and subsequently redissolved in CH_2Cl_2 for purification by silica gel chromatography with neat CH_2Cl_2 as eluent. The unreacted metal-free $(TBP)_8CzH_3$ elutes first, running close to the solvent front as a dark green band, followed by the vanadium complex, which elutes as a concentrated brown band. No other products were observed to elute from the column. Analysis by TLC revealed one spot for **1**, indicating no further purification was necessary.

(41) Czernuszewicz, R. S. *Appl. Spectrosc.* **1986**, *40*, 571−573.
(42) Walters, M. A. *Appl. Spectrosc.* **1983**, *37*, 299−300.
(43) Czernuszewicz, R. S. In *Methods in Molecular Biology*; Jones, C., Muloy, B., Thomas, A. H., Eds.; Humana Press: Totowa, NJ, 1993; Vol. 17, pp 345−374.

The vanadium complex is stable to air- or light-induced degradation for months as a solid, but a dilute (0.05 mM) solution of **1** in CH_2Cl_2 exhibited several extra spots on TLC after standing on the laboratory benchtop for 3 weeks, indicating slow decomposition in solution.

The elution of the vanadium complex under relatively nonpolar conditions, together with its solubility in a number of organic solvents (CH_2Cl_2, THF, toluene), is consistent with its formulation as an overall neutral species. For **1** to be a neutral $V^{IV}(O)$ complex, the Cz ligand must be serving as a −2 donor, with a single proton remaining attached either at a *meso*-N or pyrrole-N position. A previously reported vanadium(IV)−oxo corrole complex was also formulated as a neutral complex with one proton remaining attached to the macrocycle, $V^{IV}O(HL)$ (L = 2,3,7,8,12,13,17,18-octamethylcorrole).[40] This formulation was based in part on the related titanyl complex TiO(HL), in which the labile proton was identified by ^{1}H NMR spectroscopy. The labile proton in the vanadyl complexes $V^{IV}O(HL)$ and **1** cannot be observed directly by ^{1}H NMR spectroscopy because of the paramagnetism of these compounds. However, infrared spectroscopy and UV−vis data (vide infra) for **1** confirm the presence of a labile proton.

The copper complex **2** was prepared via addition of a 9-fold excess of cupric acetate to a solution of $(TBP)_8CzH_3$ (0.25 mmol) in pyridine, which was then brought to reflux and allowed to stir for 1 h (Scheme 1). During this time the reaction mixture turned from the dark green color of the metal-free Cz to an intense blue-green color indicative of the copper complex. After removal of the pyridine, the copper complex was purified by chromatography on silica gel with CH_2Cl_2 as eluent. As in the case of the vanadium complex, a small amount of unreacted metal-free Cz is the first material to elute from the column, followed by a concentrated green band corresponding to the pure copper complex. This product shows one spot upon TLC analysis, indicating that further purification was not necessary. Complex **2** is quite stable toward light- or air-induced degradation under ambient conditions either in solution (e.g. CH_2Cl_2, toluene, benzene) or in the solid state for several months.

Electronic Absorption Spectra. The UV−vis spectrum of **1** is shown in Figure 1 (brown solid line), and the spectrum for **2** (green solid line) is shown in Figure 2. Both complexes exhibit electronic absorption spectra typical of metallocorrolazines,[2,3] which are dominated by intense $\pi-\pi^*$ transitions associated with an 18-π-electron, aromatic porphyrinoid ring.[44] The spectrum for **1** reveals a split Soret band with maxima at 435 and 465 nm, a Q-band centered at 710 nm, and less intense features at 550 and 660 nm, while that of **2** exhibits 440 (Soret) and 645 (Q) nm and a less intense feature at 530 nm. One hallmark of a corrolazine ring is a Soret band that is significantly red-shifted (λ_{max} > 400 nm) in comparison to the Soret band of a porphyrazine (λ_{max} < 400 mm),[45] and both compounds **1** and **2** exhibit this feature. Interestingly, the Q-band for **1** is also the farthest red-shifted

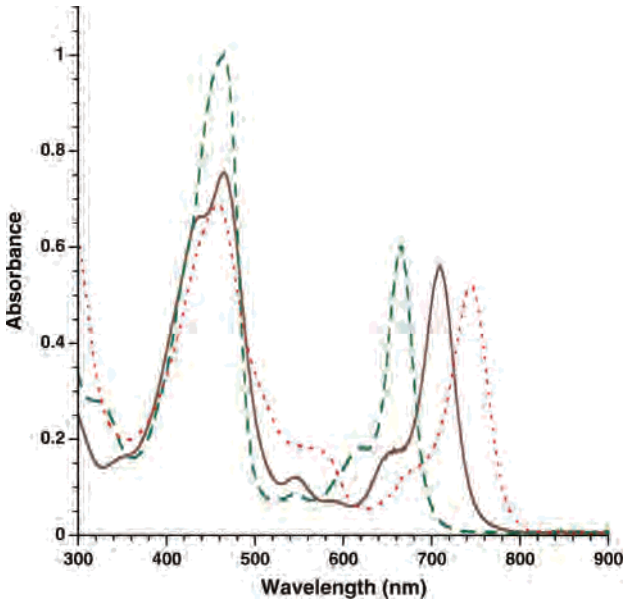

Figure 1. UV−vis spectra of $[(TBP)_8CzV^{IV}O]^-$ (green, ---), $(TBP)_8Cz(H)V^{IV}O$ (brown, —), and $[(TBP)_8Cz(H)_2V^{IV}O]^+$ (red, ···) in CH_2Cl_2.

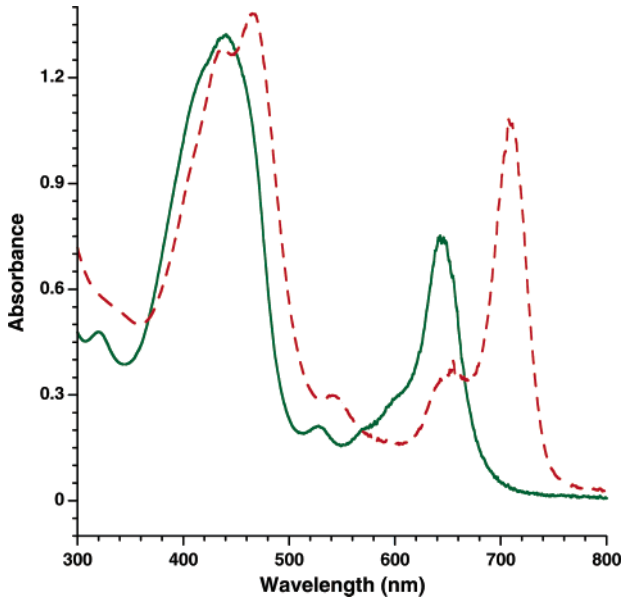

Figure 2. UV−vis spectra of $(TBP)_8CzCu^{III}$ (green, —) and $[(TBP)_8CzCu^{II}]^-$ (red, ---) in CH_2Cl_2.

in comparison to other metallocorrolazines with well-defined Q-bands.[2,3,5] The spectrum of **1** closely resembles the spectrum of $(TBP)_8CzCo(py)_2$ in the shapes and relative intensities of the peaks, including the feature at 540 nm as well as the shoulder to the shorter wavelength edge of the Q-band.[3] The former band is likely due to a charge-transfer transition, while the latter shoulder can be assigned to vibronic overtones.[46]

^{1}H NMR Spectra. The NMR spectrum of **1** shows broad, poorly defined peaks that we attribute to the paramagnetic nature of this complex. In contrast, compound **2** exhibits

(44) Mack, J.; Stillman, M. J. In *The Porphyrin Handbook*; Kadish, K. M., Smith, K. M., Eds.; Elsevier Science: San Diego, CA, 2003; Vol. 16, pp 43−116.

(45) Kobayashi, N. In *The Porphyrin Handbook*; Kadish, K. M., Smith, K. M., Guilard, R., Eds.; Academic Press: New York, 2000; Vol. 2, pp 301−360.

(46) Vagin, S.; Barthel, M.; Dini, D.; Hanack, M. *Inorg. Chem.* **2003**, *42*, 2683−2694.

sharp resonances in the diamagnetic region of the spectrum, which supports the oxidation state assignment of the copper ion as Cu(III) (square-planar, d^8). The peaks observed in the aromatic region between δ 7.15 and 8.27 ppm in CD_2Cl_2 (Experimental Section) are assigned to overlapping doublets from the four inequivalent *para*-substituted phenyl groups, and the four resonances for the unique *tert*-butyl groups appear as closely spaced singlets between δ 1.5 and 1.2 ppm. This spectrum matches that of other diamagnetic $(TBP)_8Cz$ complexes, including $[(TBP)_8CzP^V(OH)]OH$[1] and $(TBP)_8$-$CzMn^V(O)$[2] (low-spin, d^2), which have the same overall 2-fold symmetry as **2**.

Previous work has shown that the related copper corroles also exhibit clearly resolved, diamagnetic NMR spectra at room temperature, indicating a +3 oxidation state for the central copper ion.[38,39,47,48] However, variable-temperature NMR studies for some of these complexes have revealed paramagnetic behavior at higher temperatures. For example, VT-NMR studies of $(TPC)Cu^{III}$ (TPC = 5,10,15-triphenylcorrole) revealed significant line-broadening and shifting of aromatic resonances in the temperature range 300−400 K, consistent with paramagnetism.[39] In addition, similar paramagnetic effects have been observed at higher temperatures in the ^{1}H NMR spectra of $(OEC)Cu^{III}$ (OEC = 2,3,7,8,12,-13,17,18-octaethylcorrole)[47] and $[F_8T(p\text{-}CF_3\text{-}P)C]Cu^{III}$ (F_8T-(p-CF_3-P)C = β-octafluoro-*meso*-tris(*p*-(trifluoromethyl)-phenyl)corrole).[48]

The paramagnetic behavior of these copper corroles at higher temperatures has been attributed to the thermal population of a relatively low-lying triplet excited state assigned to the configuration $[(corrole^{\bullet+})Cu^{II}]$. The spin state of (TPC)Cu has also been found to be solvent dependent, with a diamagnetic spectrum seen in $CDCl_3$ but a paramagnetic spectrum observed in pyridine-d_5.[39] A five- or six-coordinate complex $(TPC)Cu^{III}(py)_n$ (n = 1 or 2), which is expected to have a high-spin (d^8) paramagnetic configuration, is presumed to form in pyridine via axial ligation.

Interestingly, compound **2** does not exhibit any paramagnetic behavior by ^{1}H NMR spectroscopy at higher temperatures. In toluene-d_8, **2** shows a well-resolved, diamagnetic ^{1}H NMR spectrum at 300 K (Figure S1), and the same diamagnetic spectrum is observed at temperatures up to 400 K, as seen in Figure 3. A similar diamagnetic spectrum is observed for **2** in pyridine-d_5. Thus, the putative (corrolazine-π-cation-radical)(Cu(II)) triplet excited state is not thermally accessible up to 400 K, whereas, in the copper corroles (OEC)Cu, $[F_8T(p\text{-}CF_3\text{-}P)C]Cu^{III}$, or $(TPC)Cu^{III}$, significant paramagnetic effects are observable at this temperature. These data clearly show that the corrolazine ligand in **2** is better at stabilizing a high oxidation state copper(III) ion than the corresponding corrole ligands.

Evidence for the Labile Proton in $(TBP)_8Cz(H)VO$ (1). Upon addition of 1 equiv of base (NEt_3) to **1** in CH_2Cl_2, its UV−vis spectrum changes to that of the dashed line in Figure 1. Titration of **1** by the addition of substoichiometric amounts of Et_3N leads to good isosbestic behavior up to 1 equiv of Et_3N (data not shown). Addition of excess Et_3N (1−50 equiv) does not cause any further changes in the spectrum, and the original spectrum for **1** can be regenerated by the addition of trifluoroacetic acid. These data provide good evidence that **1** contains a titratable proton and can be interconverted with its anion $[(TBP)_8CzV^{IV}O]^-$ (**1a**), as shown in Scheme 2. If excess acid (20 equiv of CF_3COOH) is added to **1**, a third spectrum (dotted line, Figure 1) appears, which we suggest belongs to the monocationic complex $[(TBP)_8Cz(H)_2V^{IV}O]^+$ (**1b**). Addition of Et_3N readily converts **1b** back to **1**, as shown in Scheme 2.

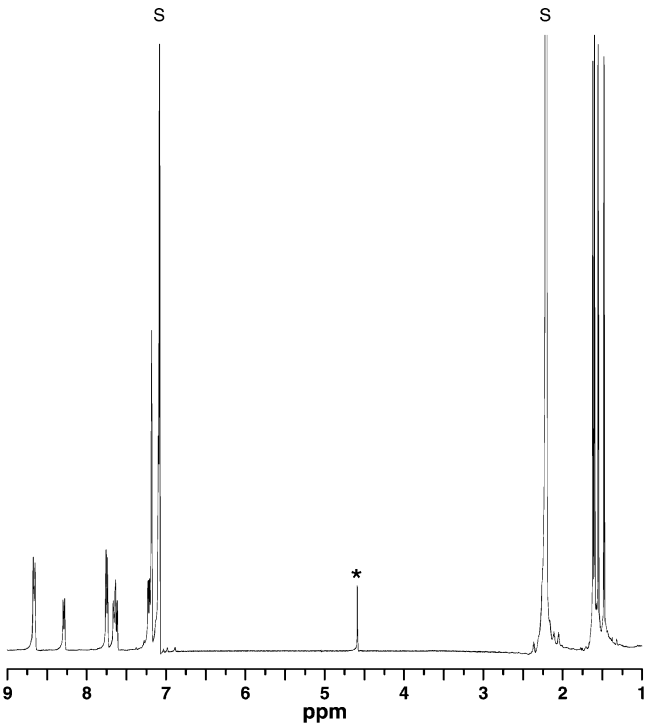

Figure 3. ^{1}H NMR spectrum of $(TBP)_8CzCu^{III}$ in toluene-d_8 at 400 K (s = solvent peaks; asterisk = impurity).

The analogous corrole compounds, $V^{IV}O(HL)$ and $Ti^{IV}O$-(HL), also show significant spectral changes upon the addition of excess base (Et_3N or OH^-), which was similarly attributed to deprotonation of a labile proton in these complexes.[40] It was suggested that the labile proton in VO-(HL) and TiO(HL) was attached to an inner pyrrole N atom on the basis of the ^{1}H NMR spectrum for the titanium complex, which revealed a peak shifted far upfield (−3.48 ppm), as expected for an internal pyrrole N−H. The site of protonation in **1** is not known, although it is possible to assign it to a pyrrole N atom by analogy with the former corrole complexes. However, the *meso* N atoms in **1**, which are not present in the analogous corroles, are reasonable alternative positions for protonation, and thus, it is not possible to conclusively assign the site of protonation at this time.

Additional evidence for the presence of the labile proton in **1** comes from IR spectroscopy. The IR spectrum of **1** reveals a strong, sharp band at 3354 cm^{-1}, which is not present in the IR spectrum of **2** (data not shown). The

(47) Will, S.; Lex, J.; Vogel, E.; Schmickler, H.; Gisselbrecht, J. P.; Haubtmann, C.; Bernard, M.; Gross, M. *Angew. Chem., Int. Ed. Engl.* **1997**, *36*, 357−361.
(48) Steene, E.; Dey, A.; Ghosh, A. *J. Am. Chem. Soc.* **2003**, *125*, 16300−16309.

Scheme 2

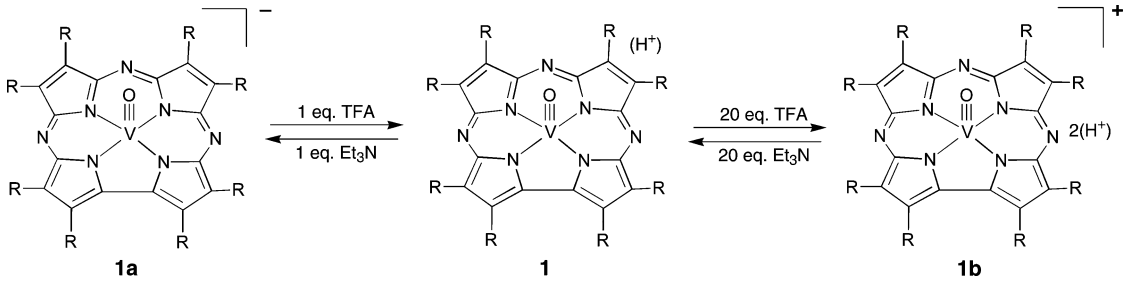

position of this band is characteristic of an N−H stretch, and a similar band has been observed in the metal-free $(TBP)_8CzH_3$, which is assigned to the $N_{pyrrole}$−H stretch (3362 cm^{-1}).[1] Thus, the IR spectrum provides direct spectroscopic proof for the presence of a labile N−H proton in the vanadyl complex, although the specific site of protonation (*meso*- versus pyrrole-N atom) remains unresolved.

Evidence for the V^{IV}≡O Bond in $(TBP)_8Cz(H)VO$ (1). Vibrational spectroscopy also provides direct evidence for the vanadium−oxo bond through its characteristic stretching peaks in the RR and IR spectra. A positive identification of these peaks is aided by their sensitivity to substitution of the oxo group with ^{18}O. The vibrational data are illustrated in Figures 4 and 5, which compare the 800−1150 cm^{-1} portions of the solid-state RR (Figure 4) and FT-IR (Figure 5) spectra of $(TBP)_8Cz(H)V^{IV}O$ and its ^{18}O isotopomer. An ^{18}O-sensitive band at 975 cm^{-1} in the RR spectrum (Figure 4a) is assigned to the vanadyl stretching vibration, ν(VO), of the vanadium(IV)−oxo moiety. Upon $^{16/18}O$ exchange this band falls under the corrolazine ligand band at 943 cm^{-1} producing a more intense band centered at ∼942 cm^{-1} (Figure 4b). The absence of the 975 cm^{-1} peak in the ^{18}O-substituted RR spectrum indicates a high level of ^{18}O incorporation. The 975 cm^{-1} frequency for the ν(VO) stretch of **1** is consistent with those previously observed at 987 cm^{-1} for $(V^{IV}O)$OEP porphyrin[42] (OEP = octaethylporphyrin) and at 970 cm^{-1} for the corrole complex $V^{IV}O(HL)$,[40] although the latter assignment was made without confirmation by isotopic exchange. The magnitude of the ^{18}O isotope shift of the ν(VO) band for **1** (∼34 cm^{-1}) is smaller than that expected for an isolated V−O diatomic oscillator (42 cm^{-1}). However, it is observed that upon ^{18}O isotopic substitution two corrolazine RR bands at 992 and 1002 cm^{-1} collapse into a broad asymmetric band centered at ∼998 cm^{-1}, indicating that ν(VO) kinematically couples to one or two of the internal corrolazine vibrations of similar frequencies. This coupling is also evident in the IR spectra where the ν(VO) stretching frequency is hidden beneath a strong corrolazine IR band at 980 cm^{-1} (Figure 5a). The ^{18}O-substituted **1** gives the $\nu(V^{18}O)$ band at 939 cm^{-1} and an upshifted (from 994 cm^{-1}) very strong corrolazine band at 997 cm^{-1} (Figure 5b). Hence, the RR and IR spectra provide complementary vibrational information with $\nu(V^{16}O)$ = 975 cm^{-1} (RR) and $\nu(V^{18}O)$ = 939 cm^{-1} (IR) and a frequency shift $\Delta\nu(^{18}O-^{16}O)$ = −36 cm^{-1}, in reasonable agreement with the calculated value (−42 cm^{-1}).[40,43,49,50]

EPR Spectrum of $(TBP)_8Cz(H)VO$ (1). The EPR spectrum of complex **1** in frozen toluene solution (77 K) is shown in Figure 6. The spectrum confirms the oxidation state

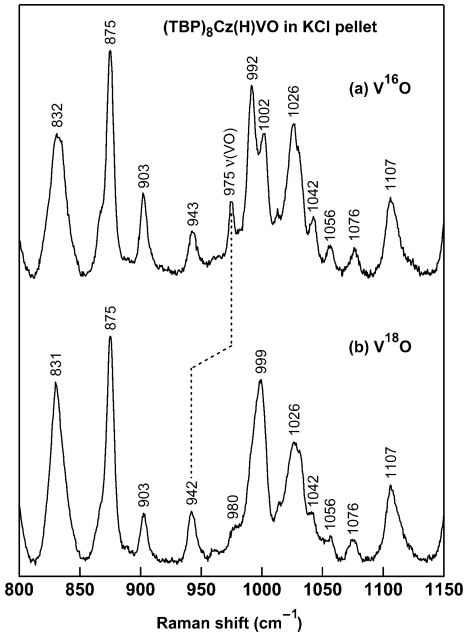

Figure 4. Resonance Raman spectra (800−1150 cm^{-1}) of (a) $(TBP)_8Cz(H)V^{IV}O$ and (b) its $V^{18}O$ isotopomer in KCl pellets obtained with 488.0 nm excitation line and 4 cm^{-1} slit widths.

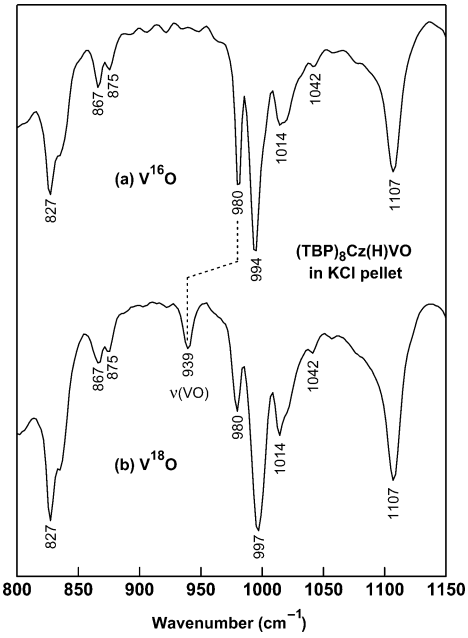

Figure 5. Infrared spectra (800−1150 cm^{-1}) of (a) $(TBP)_8Cz(H)V^{IV}O$ and (b) its $V^{18}O$ isotopomer in KCl pellets.

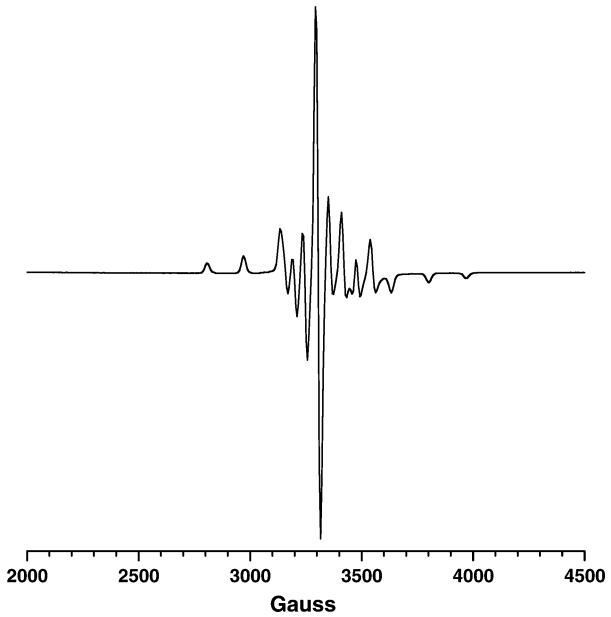

Figure 6. X-band EPR spectrum of $(TBP)_8Cz(H)V^{IV}O$ in toluene at 77 K. EPR parameters: microwave frequency, 9.478 GHz; incident microwave power, 4.72 mW; modulation frequency, 100 kHz; modulation amplitude, 1.0 G; receiver gain, 8.93×10^4.

assignment as +4, giving rise to a $V^{IV}{\equiv}O$ (d^1, $S = 1/2$) EPR spectrum. The peaks on the high-field and low-field edges of the spectrum are clearly due to the ^{51}V ($I = 7/2$) hyperfine interaction characterized by g_{zz} and A_{zz}, and a good simulation of the spectrum (Figure S2) gives $g_{xx} = 1.989$, $g_{yy} = 1.972$, $g_{zz} = 1.962$, $A_{yy} = 54.0$, $A_{xx} = 51.5$, and $A_{zz} = 153.0 \times 10^{-4}$ cm^{-1}. A direct comparison of this spectrum with that of the other vanadyl corrole $V^{IV}O(HL)$[40] cannot be made because the frozen-solution EPR spectrum for this compound was not reported. However, the spectrum for **1** is in good agreement with other $V^{IV}O$ porphyrin and non-porphyrin complexes with symmetries approximately C_{4v} and with the $V{\equiv}O$ bond defining the axial (*z*) direction.[51−55]

Chemical Reduction of $[(TBP)_8CzCu^{III}]$ To Give $[(TBP)_8CzCu^{II}]^-$ (2a). We have shown previously that $NaBH_4$ is a useful reagent for reducing $(TBP)_8CzCo^{III}(py)_2$ to the anionic cobalt(II) species $[(TBP)_8CzCo^{II}(py)]^-$.[5] This reaction is characterized by significant changes in the Q-band region of the UV−vis spectrum. Similarly, the UV−vis spectrum of **2** changes considerably upon addition of $NaBH_4$, as shown in Figure 2 (dashed line). The spectrum of **2** changes most noticeably in the Q-band region, with a

Scheme 3

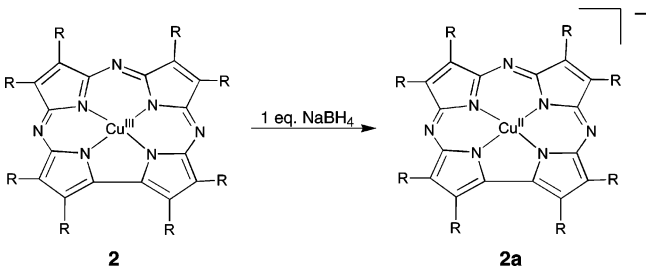

significant increase in absorption at 708 nm and concomitant decrease in the peak at 645 nm. The reduced product is assigned as the copper(II) complex $[(TBP)_8CzCu^{II}]^-$ (**2a**), as shown in Scheme 3. The formation of a copper(II) species is corroborated by EPR spectroscopy. The $(TBP)_8CzCu^{III}$ complex **2** exhibits no EPR signal, as is expected for a low-spin (d^8) Cu(III) ion, but after reduction with $NaBH_4$ to **2a** an intense EPR signal is observed, as seen in Figure 7. This

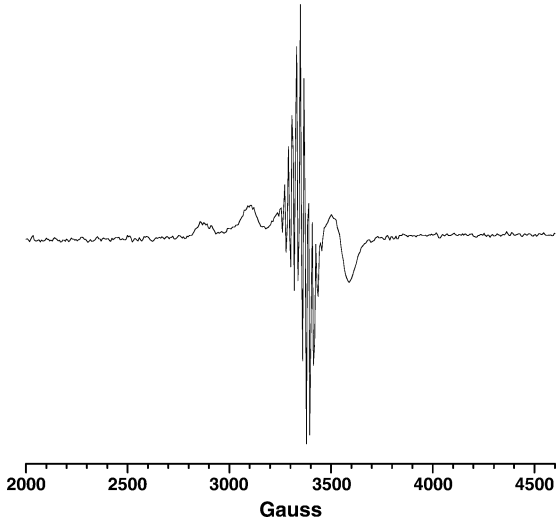

Figure 7. X-band EPR spectrum of $[(TBP)_8CzCu^{II}]^-$ in toluene at 25 K. EPR parameters: microwave frequency, 9.478 GHz, incident microwave power, 12.69 mW; modulation frequency, 100 kHz; modulation amplitude, 1.0 G; receiver gain, 1.59×10^4.

spectrum is indicative of a Cu(II) (d^9, $S = 1/2$) porphyrin[52,56,57] with characteristic hyperfine splittings from the Cu ($I = 3/2$) nucleus and superhyperfine interactions with the four pyrrole nitrogen atoms of the corrolazine ligand. A simulation of the experimental spectrum (Figure S3) yields $g_{||} = 2.062$, $g_{\perp} = 2.001$, $a_{||}^{Cu} = 227$ G, $a_{\perp}^{Cu} = 15$ G, $a_{\perp}^{N} = 19.53$ G, and $a_{||}^{N} = 17.36$ G, with the assumption of four equivalent $^{14}N_{pyrrole}$ nuclei interacting with the unpaired electron.

Previous descriptions of Cu(II) corroles are scarce. Kadish and Vogel have reported the generation of an octaalkyl-substituted Cu(II) corrole by controlled-potential reduction of $(OEC)Cu^{III}$.[38] The electroreduced product exhibited an EPR spectrum similar to **2a**, with $g_{||} = 2.192$, $g_{\perp} = 2.092$, and $a_{||} = 227$ G ($a_{\perp}^{Cu}$, $a_{||}^{N}$, and $a_{\perp}^{N}$ not determined). An

(49) Su, Y. O.; Czernuszewicz, R. S.; Miller, L. A.; Spiro, T. G. *J. Am. Chem. Soc.* **1988**, *110*, 4150−4157.
(50) Czernuszewicz, R. S.; Spiro, T. G. In *Inorganic Electronic Structure and Spectroscopy*; Solomon, E. I., Lever, A. B. P., Eds.; Wiley-Interscience: New York, 1999; Vol. 1, pp 353−441.
(51) Guilard, R.; Lecomte, C. *Coord. Chem. Rev.* **1985**, *65*, 87−113.
(52) Kadish, K. M.; Araullo, C.; Maiya, G. B.; Sazou, D.; Barbe, J. M.; Guilard, R. *Inorg. Chem.* **1989**, *28*, 2528−2533.
(53) Tolis, E. J.; Teberekidis, V. I.; Raptopoulou, C. P.; Terzis, A.; Sigalas, M. P.; Deligiannakis, Y.; Kabanos, T. A. *Chem.−Eur. J.* **2001**, *7*, 2698−2710.
(54) Tasiopoulos, A. J.; Troganis, A. N.; Deligiannakis, Y.; Evangelou, A.; Kabanos, T. A.; Woollins, J. D.; Slawin, A. *J. Inorg. Biochem.* **2000**, *79*, 159−166.
(55) Öztürk, R.; Güner, S.; Aktas, B.; Gül, A. *Synth. React. Inorg. Met.-Org. Chem.* **2001**, *31*, 1623−1630.
(56) Greiner, S. P.; Rowlands, D. L.; Kreilick, R. W. *J. Phys. Chem.* **1992**, *96*, 9132−9139.
(57) Cunningham, K. L.; McNett, K. M.; Pierce, R. A.; Davis, K. A.; Harris, H. H.; Falck, D. M.; McMillin, D. R. *Inorg. Chem.* **1997**, *36*, 608−613.

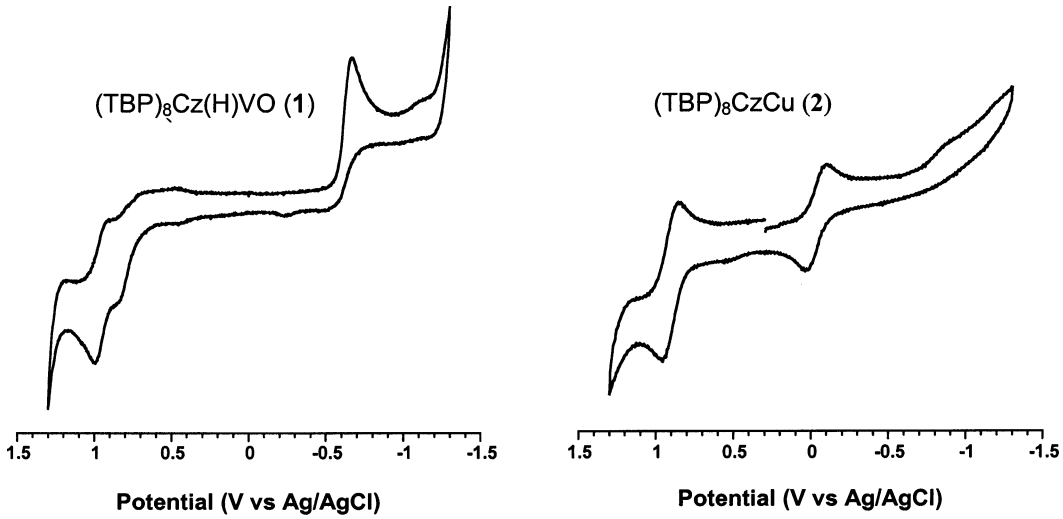

Figure 8. Cyclic voltammograms of compounds **1** and **2** in CH_2Cl_2 containing 0.1 M $(Bu_4N)PF_6$.

Table 1. Half-Wave Potentials (V vs Ag/AgCl) of Compounds **1** and **2** with Copper Corroles and Vanadyl Porphyrin

compd[a]	oxidn	redn	ref
1	0.96	−0.65 (irrev)	this work
2	0.93	−0.05	this work
[(OEC)Cu^{III}][b,c]		−0.30	38
[(TPC)Cu^{III}][b,c]	0.80	−0.16	48
[(TPFPC)Cu^{III}][b,c]	1.18	0.24	37
[(T(*p*-CF_3-P)C)Cu^{III}][b,c]	0.84	−0.12	48
[(Br_8T(*p*-H-P)C)Cu^{III}][b,c]	1.10	0.08	48
[(F_8T(*p*-H-P)C)Cu^{III}][b,c]	1.10	0.18	48
[(TPP)V^{IV}O][b,d]	0.95	−1.02	60

[a] OEC = 2,3,7,8,12,13,17,18-octaethylcorrole; TPC = 5,10,15-triphenylcorrole; TPFPC = 5,10,15-tris(pentafluorophenyl)corrole; T(*p*-CF_3-P)C = 5,10,15-tris(*p*-(trifluoromethyl)phenyl)corrole; Br_8T(*p*-H-P)C = β-octabromo-*meso*-triphenylcorrole; F_8T(*p*-H-P)C = β-octafluoro-*meso*-triphenylcorrole; TPP = tetraphenylporphyrin. [b] Values converted from V vs SCE to V vs Ag/AgCl via $E_{1/2}$ (SCE) = $E_{1/2}$(Ag/AgCl) + 0.045 V. [c] Measurement performed in CH_2Cl_2, 0.10 M TBAP. [d] Measurement performed in DMF, 0.10 M TBAP.

earlier study by Murakami also reported EPR data for copper(II) complexes of the corroles MEC and PMC (MEC = 2,3,-17,18-tetramethyl-7,8,12,13-tetraethylcorrole, PMC = 8,12-bis[2-(ethoxycarbonyl)ethyl]-2,3,7,13,17,18-hexamethylcorrole), $2.145 < g_{||} < 2.152$, $2.021 < g_{\perp} < 2.030$, $207 < a_{||}^{Cu} < 246 \times 10^{-4}$ cm^{-1}, $13.0 < a_{\perp}^{N} < 16.1 \times 10^{-4}$ cm^{-1}, and $15.6 < a_{||}^{N} < 17.3 \times 10^{-4}$ cm^{-1}, but the formulation of these compounds as "neutral" molecules with the corrole ligands serving as −2 donors calls into question the exact nature of these species.[58,59]

Electrochemistry. The cyclic voltammograms of compounds **1** and **2** are shown in Figure 8, and the half-wave potentials are presented in Table 1. The first reduction for **1** is observed at −0.65 V and is found to be irreversible over a range of scan rates (50−500 mV/s). We assign this reduction to a metal-centered process ($V^{IV} \rightarrow V^{III}$), since the observed irreversibility would be consistent with the formation of a V^{III}−oxo species that is likely to be unstable, whereas a ring-centered reduction can be expected to be a reversible process. At positive potentials there appears to be two overlapping processes, which could be either ring- or metal-centered. There are no electrochemical data available for the other vanadium−oxo corrole $V^{IV}O$(HL) for comparison, but the data for the related porphyrin complex (TPP)-$V^{IV}O$[60] (TPP = tetraphenylporphyrin) are included in Table 1 for reference. It is easier to reduce **1** than (TPP)V^{IV}O by almost 400 mV, which contrasts the more typical pattern of a corrole being more difficult to reduce than an analogous porphyrin.[11] The behavior of **1** is closer to that of porphyrazines, which are usually much easier to reduce than porphyrins because of the increased electronegativity of the *meso* nitrogen atoms.[45,61] These observations are nicely explained by the unusual protonation state of **1**; the "extra" labile proton in **1** gives an overall charge of −2 to the corrolazine, making it behave more like a porphyrazine than a corrolazine and causing **1** to be more easily reduced.

The copper corrolazine **2** exhibits two reversible waves centered at 0.93 and −0.05 V, respectively. We assign the reduction wave at −0.05 V to a Cu(III)/Cu(II) couple on the basis of the fact that chemical reduction of **2** with $NaBH_4$ gives a metal-centered reduction to generate $[(TBP)_8CzCu^{II}]^-$. Several different copper corroles have been characterized by cyclic voltammetry, and it is instructive to compare the data from some representative examples given in Table 1. These copper complexes can be divided into three categories on the basis of the peripheral substitution of the corrole ligand: substituents at the β-carbon atom (e.g., alkyl, F, Br), substituents at the *meso*-carbon atom (e.g., Ph, *para*-X-Ph, F_5Ph), or both β-carbon and *meso*-carbon atom substitution. For example, (OEC)Cu, studied in detail by Kadish and Vogel, exhibits a first reduction wave which is nearly 300 mV more negative than compound **2** (the oxidative process for this compound is complicated by intermolecular dimerization).[38] This result is not surprising, in that the eight ethyl

(58) Murakami, Y.; Matsuda, Y.; Sakata, K.; Yamada, S.; Tanaka, Y.; Aoyama, Y. *Bull. Chem. Soc. Jpn.* **1981**, *54*, 163−169.
(59) Another report of a reduced copper(II) corrole has recently appeared in the literature: Luobeznova, I.; Simkhovich, L.; Goldberg, I.; Gross, Z. *Eur. J. Inorg. Chem.* **2004**, *8*, 1724−1732.
(60) Kadish, K. M.; Sazou, D.; Araullo, C.; Liu, Y. M.; Saoiabi, A.; Ferhat, M.; Guilard, R. *Inorg. Chem.* **1988**, *27*, 2313−2320.
(61) Michel, S. L. J.; Hoffman, B. M.; Baum, S. M.; Barrett, A. G. M. *Prog. Inorg. Chem.* **2001**, *50*, 473−590.

substituents on OEC are electron-donating compared to the TBP substituents of **2** and, most importantly, the *meso*-nitrogen atoms of **2** are more electronegative than the *meso*-C atoms of (OEC)Cu. Removal of the ethyl groups and addition of electron-withdrawing phenyl substituents at the *meso* positions, as found in (TPC)Cu,[48] brings the first oxidation and reduction waves closer to those observed for **2,** but both processes are still more negative than seen for **2**. Only with full fluorination of the *meso*-phenyl groups do the half-wave potentials become more positive for a copper corrole than for **2**, as seen for (TPFPC)Cu (TPFPC = 5,10,15-tris-(pentafluorophenyl)corrole).[37] Complete bromination or fluorination at the β-carbon atom positions of (Br_8TPC)Cu and (F_8TPC)Cu also leads to slightly more positive oxidation/reduction potentials.[48] The conclusion in comparing these different types of Cu corroles to **2** is that the *meso*-N atoms of a corrolazine make it substantially more resistant to oxidation and easier to reduction than the corresponding corrole, unless the corrole bears multiple electron-withdrawing substituents at the *meso* and/or β-carbon atom positions. The significant electron-withdrawing effects of the *meso*-N atoms on the electronic properties of the corrolazine have been pointed out before.[1,3,5,62]

Conclusions

The first examples of copper and vanadium corrolazines have been prepared. Through a combination of spectroscopic and electrochemical methods (UV−vis, FT-IR, RR, EPR, cyclic voltammetry) and acid/base reactivity the vanadium complex **1** has been definitively characterized as a neutral vanadium(IV) species, with the corrolazine ligand containing a single labile proton and acting as a −2 ligand instead of the more typical, fully deprotonated −3 ligand. These findings are consistent with the only other vanadium corrole reported thus far, which was also formulated with a protonated, −2 corrole ligand and an overall neutral charge. The multiply bonded terminal oxo ligand in $(TBP)_8Cz(H)V^{IV}O$ was identified by direct observation of the vanadium−oxo stretching mode, ν(VO), in RR and IR spectra for both $V^{16}O$ and $V^{18}O$ isotopomers. The EPR spectrum for **1** is, as expected, typical of a vanadyl porphyrin-type compound, but the electrochemical data for **1** are complicated by the protonation state of the corrolazine ligand, resulting in behavior closer to that of a porphyrazine than a corrolazine. The corrolazine in the copper complex **2** serves in the normal capacity of a Cz^{3-} ligand and stabilizes the relatively high oxidation state +3 for the copper center. The ^{1}H NMR spectrum for $(TBP)_8CzCu^{III}$ is diamagnetic at room temperature as expected. Interestingly, this complex does not display a paramagnetic NMR spectrum at high temperature, in contrast to copper(III) corroles, which have a thermally accessible triplet state [(corrole$^{\bullet+}$)Cu^{II}]. It is clear from these findings that the corrolazine in **2** is behaving as an "innocent" ligand and is better for stabilizing a high oxidation state copper(III) center than a corrole ligand.

Acknowledgment. We thank the NSF (Grants CHE00-94095 and CHE0089168 to D.P.G.) and Robert A. Welch Foundation (Grant E-1184 to R.S.C) for financial support. D.P.G. is also grateful for an Alfred P. Sloan Research Fellowship.

Supporting Information Available: The simulated EPR spectra of **1** and **2** and ^{1}H NMR spectrum of **2** at 300 K. This material is available free of charge via the Internet at http://pubs.acs.org.

IC049384A

(62) Fox, J. P.; Goldberg, D. P. *Inorg. Chem.* **2003**, *42*, 8181−8191.